Stem Cell Research 37 (2019) 101443

Contents lists available at ScienceDirect

Stem Cell Research

journal homepage: www.elsevier.com/locate/scr

The role of nuclear receptors in the differentiation of oligodendrocyte precursor cells derived from fetal and adult neural stem cells

Vito Antonio Baldassarro[a,b,c,d,e,f,*], Wojciech Krężel[c,d,e,f], Mercedes Fernández[h], Brigitte Schuhbaur[c,d,e,f], Luciana Giardino[a,g,h], Laura Calzà[a,b,g]

[a] Health Science and Technologies Interdepartmental Center for Industrial Research (HST-ICIR), University of Bologna, Italy
[b] Department of Pharmacy and Biotechnology, University of Bologna, Italy
[c] Institut de Génétique et de Biologie Moléculaire et Cellulaire, Illkirch, France
[d] Inserm, U1258 Illkirch, France
[e] CNRS, UMR, 7104 Illkirch, France
[f] Université de Strasbourg, Illkirch, France
[g] IRET Foundation, Ozzano Emilia, Italy
[h] Department of Veterinary Medical Sciences, University of Bologna, Italy

ARTICLE INFO

Keywords:
Oligodendrocyte precursor cells
Thyroid hormone
Retinoic X receptor gamma
Myelination
Remyelination

ABSTRACT

Oligodendrocyte precursor cells (OPCs) differentiation from multipotent neural stem cells (NSCs) into mature oligodendrocytes is driven by thyroid hormone and mediated by thyroid hormone receptors (TRs). We show that several nuclear receptors display strong changes in expression levels between fetal and adult NSCs, with an overexpression of TRβ and a lower expression of RXRγ in adult. Such changes may determine the reduced capacity of adult OPCs to differentiate as supported by reduced yield of maturation and compromised mRNA expression of key genes. RXRγ may be the determinant of these differences, on the evidence of reduced number of mature oligodendrocytes and increased number of proliferating OPCs in RXRγ−/− cultures. Such data also points to RXRγ as an important regulator of the cell cycle exit, as proved by the dysregulation of T3-induced cell cycle exit-related genes.

Our data highlight the biological differences between fetal and adult OPCs and demonstrate the essential role of RXRγ in the T3-mediated OPCs maturation process.

1. Introduction

Oligodendrocyte precursor cells (OPCs) are progenitors deriving from multipotent neural stem cells (NSCs) that generate oligodendrocytes (OLs), the glial cells responsible for axon myelination in the central nervous system. During embryonic and early post-natal period, progression of myelination is a complex and temporally orchestrated process that includes: i) the birth, migration, and proliferation of OPC; ii) the phenotypic differentiation of OPC into myelinating OL; iii) axonal contact and generation of compact myelin and iv) trophic and metabolic support of the encased axon (Michalski and Kothary, 2015). During adult life, a substantial number of proliferating OPCs persist in the CNS, being responsible for myelin turnover, replacement and repair (Hughes et al., 2013).

The OL lineage begins with the specification of OPCs from multipotent NSCs, which in addition to OPCs also generate neurons, radial glia, astrocytes and bipotential astrocyte-oligodendrocyte progenitors that colonize the central nervous system (CNS; Goldman and Kuypers, 2015). OPCs, recognized as replicating NG2-positive progenitors, are not a homogeneous population, and give rise to diverse progenies in different brain regions and at various stages of development (Viganò and Dimou, 2016), organized in three separate waves. The final step consists of defining the entire OL population (Kessaris et al., 2006).

OPCs generated during development are distributed throughout the grey and white matter of the adult human brain and spinal cord, comprising the largest population of dividing cells in the mature CNS (Michalski and Kothary, 2015). In the healthy adult brain, new myelin is continuously generated, showing a persistent remodeling (Yeung et al., 2014). Specifically, new OPCs are generated by proliferation and

Abbreviations: NRs, Nuclear receptors; NSCs, Neural stem cells; OLs, Oligodendrocytes; OPCs, Oligodendrocyte precursor cells; T3, Triiodothyronine; TH, Thyroid hormone; TRs, Thyroid receptors

* Corresponding author at: CIRI-SDV, University of Bologna, Via Tolara di Sopra 41/E, 40064 Ozzano Emilia (Bologna), Italy.
E-mail address: vito.baldassarro2@unibo.it (V.A. Baldassarro).

https://doi.org/10.1016/j.scr.2019.101443
Received 10 December 2018; Received in revised form 10 April 2019; Accepted 16 April 2019
Available online 17 April 2019

asymmetric division from NSCs in the subventricular zone (SVZ) of the lateral ventricle (Urbán and Guillemot, 2014). This myelination - and therefore myelin volume - in humans is activity-dependent and can increase via the generation of new cells or new membrane from existing cells (Bercury and Macklin, 2015), for example when practicing new skills (Bengtsson et al., 2005) or learning a language (Schlegel et al., 2012). However, the number of OLs decreases with aging (Hill et al., 2018), possibly reflecting a reduced capacity of the remaining OPCs for oligodendrogenesis.

In addition to the spontaneous or function-dependent formation of OL formation during development and in adult life, OPCs are also essential for myelin regeneration following myelin lesion. Following demyelination insults, therefore, OPCs migrate to axons and differentiate into mature OLs (Fukushima et al., 2015), which leads to complete anatomical and functional myelin sheath restoration, thus representing a true regenerative capability of the CNS (Crawford et al., 2013). This regenerative capacity following trauma such as white matter stroke (Marin and Carmichael, 2018), however, is strongly impaired with aging due to unknown mechanisms (Dietz et al., 2016).

The process of remyelination is not carried out by pre-existing mature OLs, but involves the generation of new cells from the quiescent OPC pool distributed throughout the CNS, or from the SVZ. Different soluble factors stimulate local OPCs to switch from a quiescent state to a regenerative phenotype, in order to migrate to demyelinated areas and generate mature OLs (Bradl and Lassmann, 2010), in a process that is believed to be similar to developmental myelination (Franklin and Hinks, 1999).

The progression of OPCs through the myelination process is tightly regulated at all stages by various signals, including growth factors, protein kinases and extracellular matrix molecules, all of which influence epigenetic modifications, transcriptional and translational regulation, and the actin cytoskeleton arrangement (Bercury and Macklin, 2015).

Thyroid hormone (TH) is recognized as one of the most important factors regulating the OPC differentiation process (Billon et al., 2002, 2004; Calzà et al., 2017). Triiodothyronine (T3), the active form of TH, acts via genomic, epigenetic and non-genomic mechanisms (Lee and Petratos, 2016), inducing the OPC cell cycle exit and terminal differentiation (Durand and Raff, 2000). T3 mediates its action by binding thyroid hormone receptors (TRs; TRα and TRβ), a class of nuclear receptors (NRs) that migrate into the nucleus and regulate the expression of specific genes controlling the OPC cell cycle exit and regulating the expression of promyelinating genes (Baxi et al., 2014; Casaccia-Bonnefil and Liu, 2003). Other NRs are also involved in OPC differentiation. In particular, RXRγ (Retinoic X Receptors gamma) has been shown to be a positive regulator of the differentiation process during developmental oligodendrogenesis (de la Fuente et al., 2015), and during remyelination (Huang et al., 2011). In such activities, RXRγ may possibly act as a TR/RXR heterodimer (Lee and Privalsky, 2005), although heterodimers with a vitamin D receptor have also been suggested (de la Fuente et al., 2015). It is not known, however, whether changes in the activity of RXRγ or its partner(s) underlie the age difference in OPC differentiation.

In order to examine the potential contribution of TRs and RXRs in fetal vs adult OPC differentiation, we first explored the differences in expression/signaling of NRs in NSCs derived from the two systems, and tested the relevance of such changes in T3-mediated differentiation of OPCs, mimicking the physiological process to explore the role of TR signaling and differentiation of RXRγ−/− OPCs as a genetic approach to address the involvement of RXRγ.

2. Materials and methods

2.1. Cell cultures

All animal protocols described herein were carried out according to the European Community Council Directives (86/609/EEC) and complied with the guidelines published in the *NIH Guide for the Care and Use of Laboratory Animals*.

Fetal and adult NSCs were isolated from E13.5 fetal forebrain or 2.5-month-old adult SVZ (Alhenius and Kokaia, 2010) and induced for OL lineage differentiation (Chen et al., 2007). Cells were isolated from C57BL/6 J mice (Jackson) or RXRγ+/+ and RXRγ−/− mice raised on mixed C57BL/6 J × 129SV pass genetic background (Krezel et al., 1996).

Tissues were mechanically and enzymatically (trypsin 1.33 mg/ml, hyaluronidase 0.7 mg/ml, DNase 80 U/ml; Sigma-Aldrich) dissociated. After centrifugation and washing, the cellular pellet was resuspended in a serum-free medium (DMEM/F12 GlutaMAX 1 x; 8 mmol/L HEPES; 100 U/100 µg Penicillin/Streptomycin; 0.1 x B27; 1 × N-2; 20 ng/ml bFGF; 20 ng/ml EGF). Cells were plated in suspension at a density of 10 cells/µl. Half medium was changed every three days. Neurospheres were allowed to proliferate until they attained a diameter of approximately 100 µm.

To obtain the secondary neurospheres, the primary neurospheres were centrifuged, the pellet was mechanically dissociated by pipetting, and the cells were counted and plated again at a density of 10 cells/µl under the same conditions. At the same time, to obtain the oligospheres, the single cell cultures were plated in OPC medium (DMEM/F12 GlutaMAX 1 x; 8 mmol/l HEPES; 100 U/100 µg Penicillin/Streptomycin; 0.1 × B27; 1 × N-2; 20 ng/ml bFGF; 20 ng/ml PDGF). The oligospheres were centrifuged and the pellet was mechanically dissociated to obtain a single cell suspension. After the cell count, the cells were plated at a density of 3000 cells/cm^2 on poly-D,L-ornithine (50 µg/ml)/laminin (5 µg/ml) coating, in OPC medium.

To induce OL differentiation and maturation, after 3 DIVs, the OPC medium was replaced with OL differentiation medium (DMEM/F12 GlutaMAX 1 x; 8 mmol/l HEPES; 100 U/100 µg Penicillin/Streptomycin; 0.1 × B27; 1 × N-2; 50 nM T3; 10 ng/ml CNTF; 1 × *N*-acetyl-L-cysteine -NAC-).

2.2. RNA isolation and reverse transcription

Total RNA isolation was performed with the RNeasy Mini kit (Qiagen) following the manufacturer's instructions. The total RNA was eluted in RNase-free water and the concentration estimated by Nanodrop 2000 spectrophotometer (Thermo Scientific). First strand cDNAs were obtained using the iScript™ cDNA Synthesis Kit (Bio-Rad), incubating at 42 °C for 30 min. An RNA sample with no reverse transcriptase enzyme in the reaction mix was processed as a no-reverse transcription control sample.

2.3. PCR array

The RNeasy Micro Kit (Qiagen) was used for total RNA extraction, and 300 ng were retrotranscribed using the RT^2 First Strand Kit (Qiagen), following the manufacturer's instructions.

For the study of NSCs gene expression, a PCR array for nuclear receptors and co-regulators was used in combination with the RT^2 SYBR Green qPCR Mastermix (Qiagen), using 10 ng of cDNA per well. A pool of three independent culture preparations was used.

STRING software (version 10.0; European Molecular Biology Laboratory, Heidelberg, Germany; https://string-db.org/) was used to analyze the protein-protein interaction of proteins derived from the genes differentially expressed in fetal and adult NSCs (fold of difference < 2). The STRING database provides interaction information from different panels, including protein and PubMed queries, connecting proteins in clusters according to their interactions and their involvement in biological processes. To analyze the strength of the protein interactions, the default options were used (minimum confidence, 0.400). The proteins were processed using the undirected edges method. STRING software allows the identification of the net of

interactions, including other proteins closely linked to the one analyzed, in order to gain a better understanding of the possible pathways involved in the differentially expressed genes. The position in the net is dependent on the number and the strength of the interactions between the investigated proteins.

2.4. Semi-quantitative real-time PCR

Semi-quantitative real-time PCR was performed using the CFX96 real-time PCR system (Bio-Rad, CA, USA). The reactions were performed in a final volume of 20 µl, consisting of 1× SYBR Green qPCR master mix (Bio-Rad) and 0.4 µM forward and reverse primers. In order to avoid possible contamination of genomic DNA in isolated RNA, the sample with no-reverse transcriptase enzyme was processed in parallel with the others and tested by real-time PCR for every pair of primers used. All primers used were designed using Primer Blast software (NCBI, MD, USA), and synthesized by IDT (Coralville, IA, USA). The primer sequences are listed in Table S1 (Supplemental material). GAPDH was used as housekeeping gene to normalize the amount of reverse-transcribed RNA used for PCR. The thermal profile of PCR reactions initially consisted of a denaturation step (95 °C, 2 min), followed by 40 cycles of amplification (95 °C for 15 s and 60 °C for 60 s). At the end of the amplification cycles, the melting curve of amplified products was performed according to the following temperature/time scheme: heating from 55 °C to 95 °C with a temperature increase of 0.5 °C/s. The $2^{(-\Delta\Delta CT)}$ method was used for the calculation of gene expression.

2.5. Immunocytochemistry

Indirect immunofluorescence was used to identify OPCs (NG2- and PDGFαR), mature (CNPase- and APC) and myelinating (MBP) OLs, neurons (β-III-tubulin), astrocytes (GFAP), replicating cells (Ki67), and Olig1 and Olig2 expressing cells.

Although no co-culture experiments were performed to functionally prove the efficiency of fetal and adult myelination, we used “mature” and “myelinating” OLs to discriminate between CNPase-only and CNPase/MBP-positive cells.

The list of antibodies is shown in Table S2 (Supplemental materials). After immunofluorescence staining, cells were incubated with the nuclear dye Hoechst 33258 (1 µg/mL in PBS, 0.3% Triton-X 100) for 20 min at RT. Finally, the cells were washed in PBS and mounted in glycerol and PBS (3:1, *v*/v) containing 0.1% paraphenylenediamine.

2.6. Confocal microscopy

Confocal microscopy was used to study the culture lineage composition of RXRγ+/+ and RXRγ−/− cultures. Slides were scanned with a Nikon Ti-E fluorescence microscope coupled to an A1R confocal system (Nikon). A diode laser system with a 405 nm wavelength output, an air-cooled Argon-Ion laser system with a 488 nm wavelength output, a yellow diode-pumped solid-state laser system with a 561 nm wavelength output, and a high-performance diode laser system with a 638 nm wavelength output were used. Images were acquired using a 20× lens with an optical resolution of 0.18 µm, using Nis-Elements AR 3.2 software. All the z-stacks were collected in compliance with optical section separation (z-interval) values suggested by Nis-Elements AR 3.2 software (1 µm). Major intensity projections were used for image analysis.

The percentages of APC-, MBP- and NG2-positive cells were quantified based on the total number of cells identified by the nuclear staining. The OPC/OL populations were identified using the APC/Olig1/Olig2 triple staining technique (Nakatani et al., 2013). Moreover, the effect of the RXRγ gene knock out on the cell cycle was analyzed by the percentage of double positive PDGFαR+/Ki67+ cells (replicating OPCs), calculated on the total number of PDGFαR-positive cells. Five random fields per slide (duplicate per sample) were used for the analysis.

2.7. High content screening

For HCS analysis, cells were grown in 96 flat-bottom well HCS plates (NUNC). Analysis of the condensed nuclei, cell number and lineage/differentiation markers were performed with Cell Insight™ CX5 High Content Screening (HCS; Thermo Scientific), using the *Compartmental analysis* BioApplication. Based on nuclear staining, the software is able to recognize nuclei and calculate the percentage of high intensity/small sized condensed nuclei. Moreover, based on the nuclei identified, the software is able to detect the presence of the marker-specific stain in the cell body, calculating the percentage of immunoreactive cells. Lineage/differentiation marker analysis was only performed on cells showing intact nuclei, excluding condensed nuclei from the percentage calculation.

2.8. Statistical analysis

The data is reported as mean ± SEM. Prism software (GraphPad) was used for statistical analyses and graph generation. Student's *t*-test, one-way ANOVA or two-way ANOVA and Dunnett's multiple comparison post-hoc were used to analyze the data. The results were considered significant when the probability of their occurrence as a result of chance alone was < 5% ($P < 0.05$).

3. Results

3.1. TRβ and RXRγ are differentially expressed in fetal and adult neurospheres

To study the molecular mechanisms underlying the differences between fetal and adult OPC lineages and their differentiation, we first analyzed the expression of NRs and co-regulators as transcriptional determinants of stemness and differentiation programs in very early precursors. For this purpose, we performed qPCR analyses in secondary neurospheres obtained from the fetal forebrain and adult SVZ. The proliferation protocol is shown in Fig. 1A, while the investigated genes are listed in Table S3 (Supplemental material).

We analyzed the expression data by comparing adult- to fetal-derived NSC gene expression, expressed as fold of increase. We found that adult NSCs display a general up-regulation of NRs and co-regulators compared to fetal cells (Fig. 1B). Genes showing a difference in expression equal or higher than 2 folds were considered as differentially expressed. Of all NRs and co-regulators, twenty-eight (Fig. 1C, in red) are more expressed, and 3 genes (Fig. 1C, in green) are less expressed in the adult NSCs. The list of all differentially regulated genes is also included in the figure (Fig. 1D). Different genes related to androgens (*Ar*, *Med12*, *Med13* and *Nr1i3*), estrogen (*Ncoa6*), glucocorticoids (*Ncoa6* and *Nr3c1*), vitamin D (*Med12* and *Med13*), steroid hormones (*Nr1d1*, *Nr1h3*, *Nr2c1*, *Nr2f2*, *Nr3c2*, *Ppara*, *Rarg*, *Rora*, *Rxra*, *Thrb*), retinoic acid receptors (*Ncoa6*, *Rarg*, *Rxra* and *Rxrg*) and, in particular to THs (*Med12*, *Med13*, *Ncoa4*, *Nr1d1*, *Nr1h3*, *Nr1i3*, *Trip4* and *Thrb*), are differentially regulated in adult compared to fetal cells. In particular, *TRβ* (*Trhb*) and *RXRγ* (*Rxrg*), two key genes involved in OPC differentiation, are differentially expressed NRs in adult compared to fetal OPCs: *TRβ* is 12.52 folds more expressed, while *RXRγ* is 9.27 folds less expressed in adult compared to fetal NSCs.

The network of functional or physical interactions between the proteins encoded by differentially regulated genes were analyzed by the STRING software. All the proteins encoded by the differentially regulated genes appeared as functionally interconnected, suggesting that they regulate the same developmental process in a parallel or sequential manner. Importantly, TRβ (Thrb) occupied a central part of such an interaction network, indicating that its upregulation is not only a

A

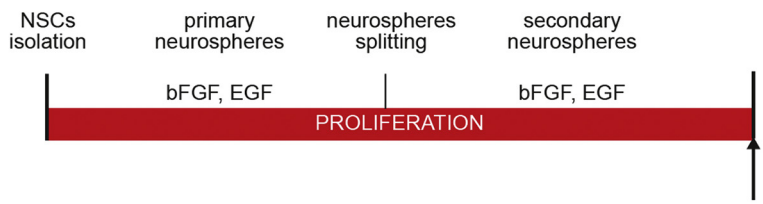

B

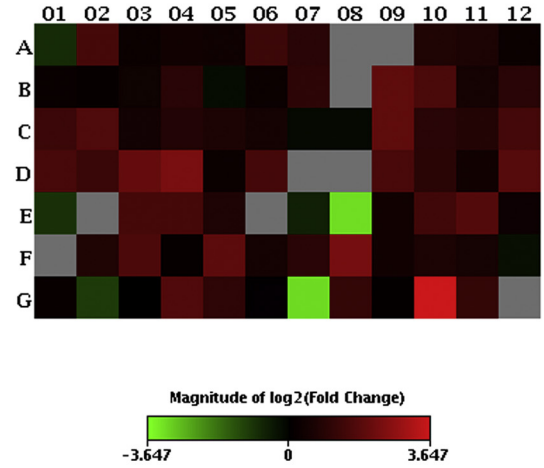

C

Layout	01	02	03	04	05	06	07	08	09	10	11	12
A	Ahr -1.72	Ar 2.88	Arnt 1.18	Brd8 1.33	Cops2 1.27	Crebbp 2.56	Ddx5 1.93	Esr1 -1.34	Esr2 -1.34	Esrra 1.69	Esrrb 1.57	Esrrg 1.19
B	Hdac1 1.13	Hdac2 1.08	Hdac3 1.25	Hdac4 1.94	Hdac5 -1.13	Hdac6 1.18	Hdac7 2.02	Hnf4a -1.34	Itgb3bp 3.91	Kat2b 3.05	Kat5 1.39	Med1 1.94
C	Med12 2.49	Med13 3.20	Med14 1.37	Med16 1.75	Med17 1.60	Med24 1.41	Med4 -1.07	Mta1 -1.08	Ncoa1 3.91	Ncoa2 1.94	Ncoa3 1.77	Ncoa4 2.78
D	Ncoa6 2.94	Ncor1 2.46	Ncor2 4.13	Nfkb2 5.27	Nono 1.19	Notch2 2.82	Nr0b1 -1.34	Nr0b2 -1.34	Nr1d1 2.96	Nr1d2 1.98	Nr1h2 1.33	Nr1h3 3.50
E	Nr1h4 -1.84	Nr1i2 -1.34	Nr1i3 2.86	Nr2c1 2.86	Nr2c2 1.63	Nr2e3 -1.34	Nr2f1 -1.48	Nr2f2 -9.40	Nr2f6 1.31	Nr3c1 2.67	Nr3c2 3.45	Nr4a1 1.22
F	Nr5a1 -1.34	Nr6a1 1.67	Nrip1 3.11	Pgr 1.06	Ppara 3.85	Ppard 1.40	Pparg 1.91	Ppargc1a 5.05	Ppargc1b 1.31	Psmc3 1.57	Psmc5 1.43	Rara -1.18
G	Rarb 1.11	Rarg -2.08	Rbpj -1.00	Rora 3.29	Rxra 2.07	Rxrb 1.03	Rxrγ -9.27	Tgs1 2.28	Thra 1.03	TRβ 12.52	Trip4 2.28	Vdr -1.34

DOWN-REGULATED GENES
UP-REGULATED GENES

D

Symbol	Description
Ar	Androgen receptor
Crebbp	CREB binding protein
Hdac7	Histone deacetylase 7
Itgb3bp	Integrin beta 3 binding protein (beta3-endonexin)
Kat2b	K(lysine) acetyltransferase 2B
Med12	Mediator of RNA polymerase II transcription, subunit 12 homolog (yeast)
Med13	Mediator complex subunit 13
Ncoa1	Nuclear receptor coactivator 1
Ncoa4	Nuclear receptor coactivator 4
Ncoa6	Nuclear receptor coactivator 6
Ncor1	Nuclear receptor co-repressor 1
Notch2	Notch gene homolog 2 (Drosophila)
Nr1d1	Nuclear receptor subfamily 1, group D, member 1
Nr1h3	Nuclear receptor subfamily 1, group H, member 3
Nr1i3	Nuclear receptor subfamily 1, group I, member 3
Nr2c1	Nuclear receptor subfamily 2, group C, member 1
Nr2f2	Nuclear receptor subfamily 2, group F, member 2
Nr3c1	Nuclear receptor subfamily 3, group C, member 1
Nr3c2	Nuclear receptor subfamily 3, group C, member 2
Nrip1	Nuclear receptor interacting protein 1
Ncor2	Nuclear receptor co-repressor 2
Nfkb2	Nuclear factor of kappa light polypeptide gene enhancer in B-cells 2, p49/p100
Ppara	Peroxisome proliferator activated receptor alpha
Ppargc1a	Peroxisome proliferative activated receptor, gamma, coactivator 1 alpha
Rarg	Retinoic acid receptor, gamma
Rora	RAR-related orphan receptor alpha
Rxra	Retinoid X receptor alpha
Rxry	Retinoid X receptor gamma
Tgs1	Trimethylguanosine synthase homolog (S. cerevisiae)
TRβ	Thyroid hormone receptor beta
Trip4	Thyroid hormone receptor interactor 4
Gusb	Glucuronidase, beta

E

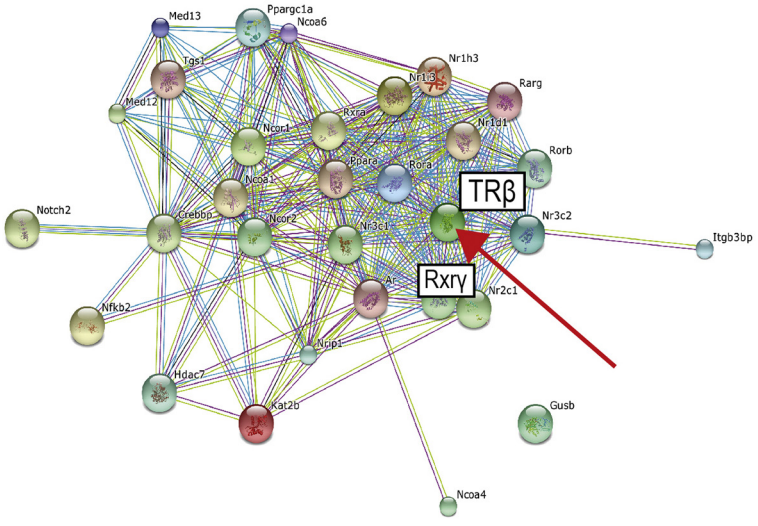

Fig. 1. Nuclear receptors and co-regulators in adult vs. fetal neurospheres.
(A) Experimental design: to study nuclear receptor and co-regulator expression in fetal and adult early precursors, secondary neurospheres were lysed and mRNA expression was analyzed using PCR array technology.
(B) Heat Plot representation of the entire array, showing the expression of adult vs. fetal neurospheres. Fold of change is expressed using a color code from green (down-regulated) to red (up-regulated); see also Table S3.
(C) Plate scheme showing the up-regulated (red) and down-regulated (green) genes (fold of change > 2).
(D) Gene list of the differentially expressed genes (fold of change > 2).
(E) Graph of the STRING software interaction analysis. Proteins encoded by the differentially expressed genes were analyzed by the STRING software to study the interaction net. In the center of the net, the TRβ is highlighted by the red arrow. (For interpretation of the references to color in this figure legend, the reader is referred to the web version of this article.)

hallmark of age-dependent changes in OPC lineage, but may also be the major coordinator of interactions between remaining NRs and their co-regulators (red arrow, Fig. 1E). Among downregulated genes, such a position could be attributed to RXRγ, which also displayed a strong interaction with TRβ. (For interpretation of the references to color in this figure legend, the reader is referred to the web version of this article.)

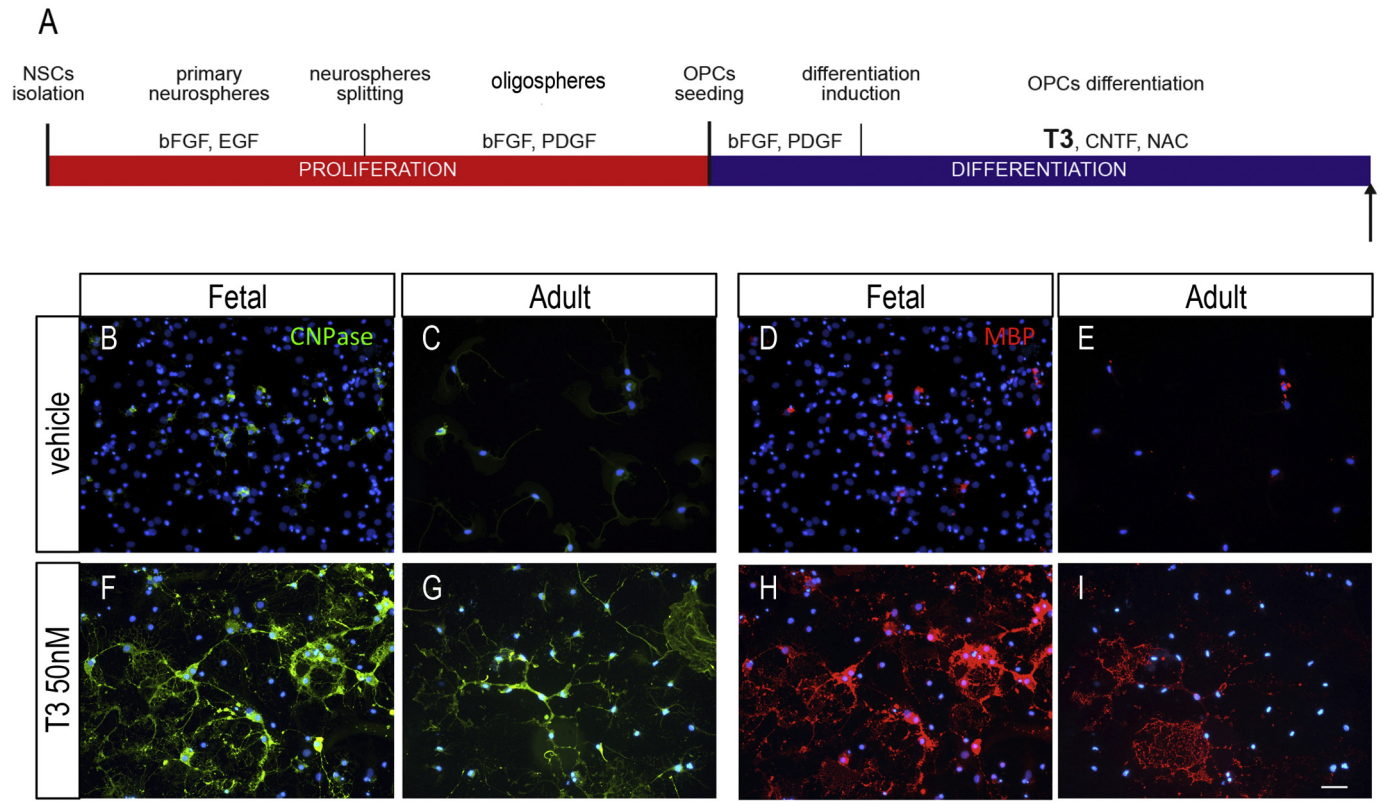

Fig. 2. T3-driven fetal and adult NSC-derived OPCs differentiation in mature OLs.
(A) Experimental design: 3 DIVs after OPC seeding, cells were exposed to vehicle (DMSO) or T3 (50nM). At the end of the differentiation phase (12 DIV) cells were stained for mature OLs markers (arrow).
(B-E) Images show the vehicle treated groups, stained for CNPase (B, C) and MBP (D, E) markers, in fetal (B, D) and adult (C, E) cultures.
(F-I) Images show the T3 treated groups, stained for CNPase (F, G) and MBP (H, I) markers, in fetal (F, H) and adult (G, I) cultures. Bar: 20 μm.
Abbreviations: CNPase, 2′,3′-cyclic nucleotide 3′-phosphodiesterase; MBP, myelin basic protein.

3.2. Fetal and adult NSCs-derived OPCs need T3 to differentiate in mature OLs

An enhanced *TRβ* expression in adult OPCs may suggest an increased sensitivity of adult OPCs to differentiation induced by T3, the well-known inducing agent of NSC differentiation to OPCs. Fetal and adult NSC cultures were differentiated as described (Fig. 2A), and the lineage progression analyzed by counting the number of differentiated cells, using CNPase as marker for pre-myelinating OLs, and MBP as marker for myelinating OLs. Both cultures needed T3 to differentiate into mature/myelinating CNPase-/MBP- positive OLs. In fact, in the absence of T3, very few CNPase and MBP-positive cells are observed, compared to T3-exposed cultures (Supplemental Fig. S1). Images showing vehicle- and T3-treated cultures at the end of the differentiation process are shown in Fig. 2B–I.

3.3. Adult NSCs-derived OPCs have the same expression pattern of OLs markers as fetal-derived OPCs, but have a different yield of maturation

To examine the molecular steps involved in the differentiation process in adult and fetal-derived OPCs, we analyzed the expression of five key differentiation genes (*Olig1*, *Olig2*, *Klf9*, *TRα* and *TRβ*) at different points of the OPC differentiation process, from neurospheres to myelinating OLs (Fig. 3A). These genes are regulators of the cell cycle exit and of the maturation of OLs, and are closely functionally connected.

Olig1, *Olig2*, *Klf9*, *TRα* and *TRβ* mRNA expression level is regulated in time and differentially expressed between the two cultures (two-way ANOVA: *Olig1*, time, $p < 0.0001$, age, $p = 0.0021$, interaction, $p < 0.0001$; *Olig2*, time, $p < 0.0001$, age, $p = 0.0035$, interaction, $p < 0.0001$; *Klf9*, time, $p < 0.0001$, age, $p < 0.0001$ interaction, $p < 0.0001$; *TRα*, time, $p = 0.0143$, age, $p < 0.0001$, interaction, $p = 0.0002$; *TRβ*, time, $p < 0.0001$, age, $p = 0.0127$, interaction, $p = 0.0006$). In particular, adult cultures show a higher expression of *Olig1*, *Olig2*, Klf9 and *TRβ* at the neurosphere and oligosphere stage (*Olig1*, neurospheres $p < 0.0001$, oligospheres $p < 0.0001$; *Olig2*, neurospheres $p < 0.0001$, oligospheres $p < 0.0001$; *Klf9*, neurospheres $p < 0.0001$, oligospheres $p < 0.0001$; *TRβ*, neurospheres $p < 0.0001$, oligospheres $p = 0.0229$; Fig. 3B–F), indicating a higher propensity to differentiate.

However, at later stages of differentiation, at OPC level (0 DIV) and after T3-induced differentiation (6 and 12 DIVs), fetal cells are more responsive to differentiation stimuli, showing a higher expression of *Olig1* at 6 DIV ($p < 0.0001$), Olig2 and *TRα* at all the differentiation time points studied (*Olig2*, 0 DIV, $p = 0.0001$, 6 DIV, $p < 0.0001$, 12 DIV, $p = 0.0248$; *TRα*, 0 DIV, $p = 0.001$; 6 DIV, $p < 0.0001$, 12 DIV, $p = 0.0128$). Notably, even if *Klf9* expression is higher in adult cells at early stages (0DIV, $p < 0.0001$), *Klf9* expression reaches higher levels in the fetal cultures at later stages (6 DIV, $p = 0.0111$; 12 DIV, $p = 0.0007$; Fig. 3D), after T3 exposure.

Notably, RXRγ expression, which resulted as being higher in fetal compared to adult neurospheres, is still higher in fetal OLs at the end of the differentiation phase (Student's *t*-test, $p = 0.0326$; Fig. 3G).

We then analyzed how these expression profiles of transcriptional determinants of OPC differentiation correlate with the actual differentiation of OPCs. To this end, we investigated markers of differentiation during the differentiation/maturation process (0, 6 and 12 DIV; Fig. 4A), i.e. PDGFαR and NG2 for OPCs, CNPase for mature OLs, MBP

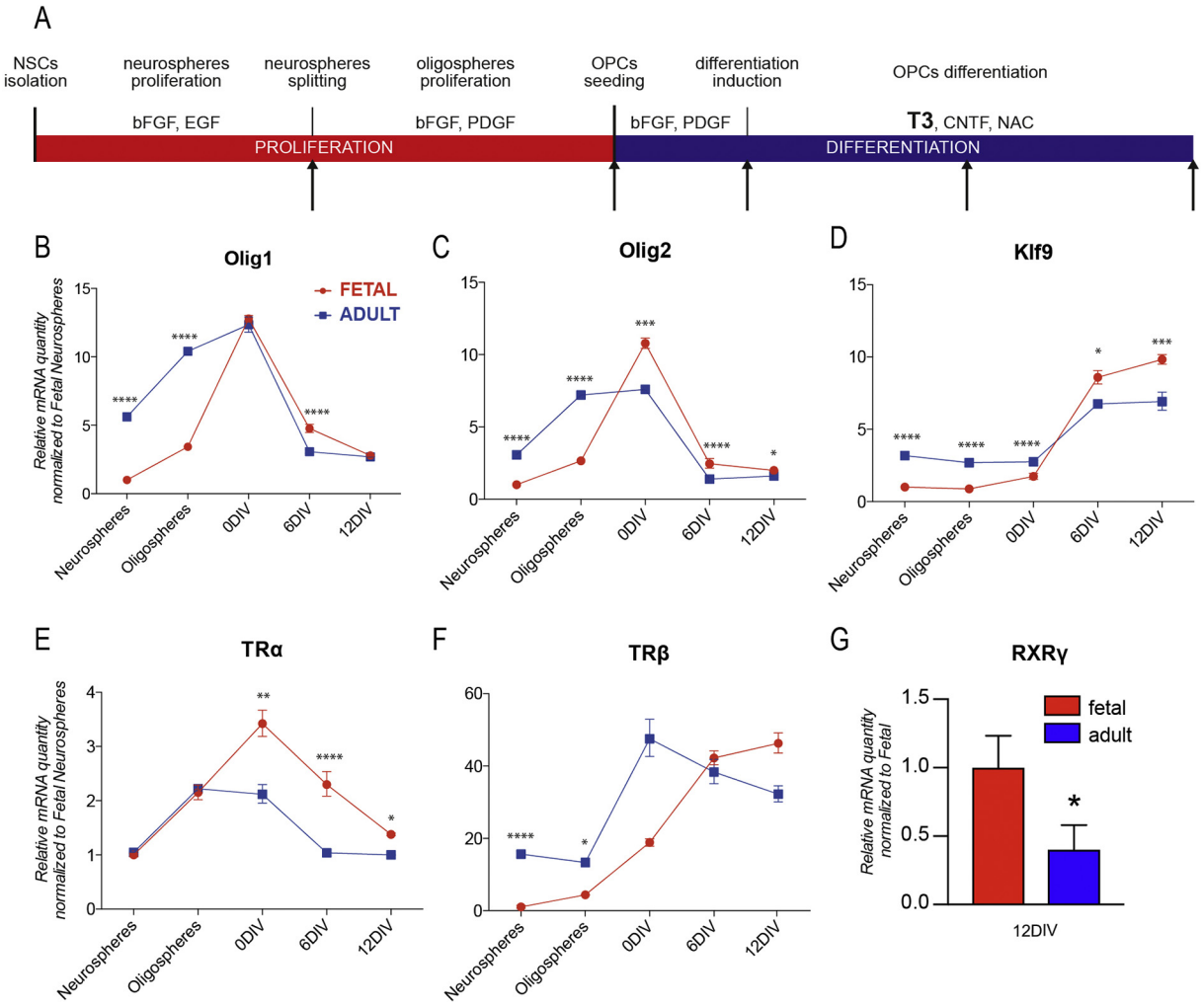

Fig. 3. Gene expression in fetal and adult NSC-derived OPCs.

(A) Experimental design: gene expression was analyzed throughout the entire differentiation process, from early progenitors to mature OLs. The arrows show the time point of the analysis: neurospheres, oligospheres, 0 DIV (before the T3 differentiation induction), 6 DIV, 12 DIV.

(B-F) Gene expression analysis of five key genes involved in the differentiation process: Olig1 (B), Olig2 (C), Klf9 (D), TRα (E) and TRβ (F). Results are shown as fold of changes of all fetal and adult time points, normalized on fetal neurospheres.

(G) Gene expression of RXRγ in differentiated/mature fetal and adult oligodendrocytes at the end of the differentiation phase (12 DIV). Results are shown as fold of changes, normalized on fetal gene expression.

The bars represent the mean value ± SEM; n = three independent experiments. Statistical analysis: Two-way ANOVA followed by Tukey's post-hoc (B-F) or Student's *t*-test (G). The asterisks represent the differences in expression at the same time point between fetal and adult cultures (* $P < 0.5$; ** $P < 0.1$; *** $P < 0.01$; **** $P < 0.001$).

Abbreviations: Klf9, Krűppel-like factor 9; Olig1, Oligodendrocyte transcription factor 1; Olig2, Oligodendrocyte transcription factor 2; RXRγ, Retinoid X receptor gamma; TRα, Thyroid hormone receptor alpha; TRb, thyroid hormone receptor beta.

for myelinating OLs, but also GFAP for astrocytes and beta-III-tubulin for neurons, to determine the specificity of NSC differentiation to OLs.

Globally, the percentage of undifferentiated OLs identified by PDGFαR or NG2 decreased more during differentiation of fetal as compared to adult OLs, indicating an enhanced differentiation of fetal OPCs by a higher percentage of CNPase and MBP cells. Specifically, according to the progress of differentiation, the percentage of PDGFαR-positive cells varied by culture time in differentiating fetal and adult OPCs (time, $p = 0.0108$, F (2,24) = 5.499), but in an opposite manner (interaction for time and age, $p < 0.0001$), with a decrease in fetal cultures at 6 DIV (0 vs. 6 DIV, $p = 0.0006$), and an increase during the same period in the adult-derived OPCs (0 vs. 6 DIV, $p = 0.0007$), but reaching the same percentage at the end of differentiation (12 DIV; Fig. 4B–D). However, NG2-positive cell percentage is affected by both time and age (time, $p = 0.0029$, F (2,24) = 7.516; age, $p = 0.0058$, F (2,24) = 9.159; Fig. 4E–G). The number of mature, CNPase-positive OLs displayed significant changes in culture time that differed depending on whether OPCs were originating from fetal or adult material (time in culture x age interaction, F (2,24) = 2.64; $p = 0.001$; Fig. 4H–J). This difference in the evolution of OL differentiation reflected increasing amounts of CNPase-positive cells in fetal cultures, compared to a decrease of those cells in adult cultures. In line with this observation, the percentage of MBP-positive cells, corresponding to mature myelinated OLs, also displayed a different evolution in time depending on age (time in culture x age interaction, $p = 0.0007$; F (2,24) = 9.987), with a significantly lower percentage of differentiated cells in adult-derived cultures at the end of the differentiation process compared to fetal-derived cells (12 DIV, $p = 0.0020$; Fig. 4K–M). A strong age effect was also observed ($p < 0.0001$; F (2,24) = 32.66). In addition, cells derived from fetal NSCs displayed a more mature phenotype compared to cells derived from adult NSCs, as illustrated by MBP-IR (Fig. 4L and M).

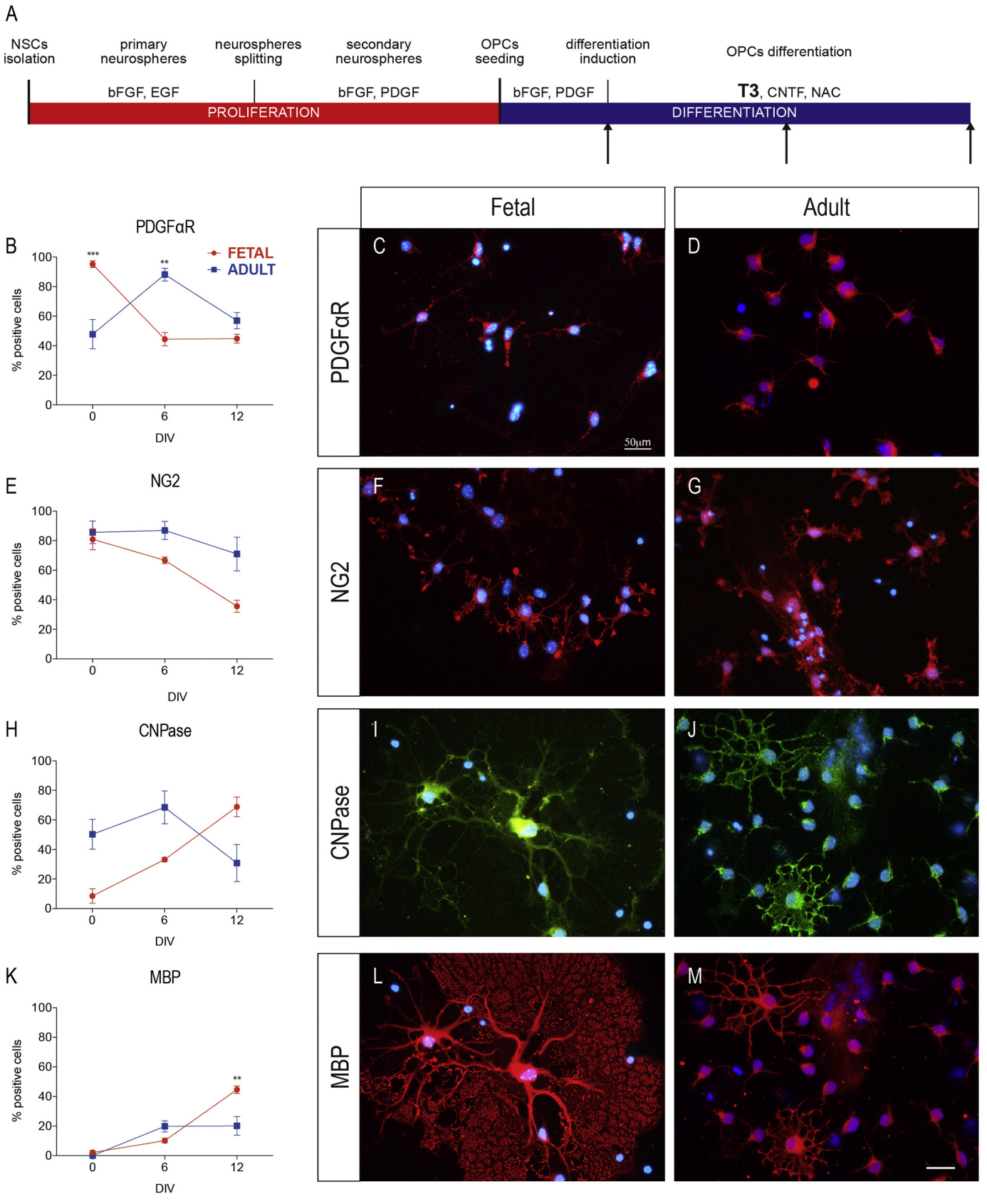

(caption on next page)

Fig. 4. OL differentiation markers in fetal and adult NSCs-derived OPCs.
(A) Experimental design: cell morphology and OPC/OL marker expression were analyzed during the differentiation process. The arrows show the time point of the analysis: 0 DIV (before the T3 differentiation induction), 6 DIV, 12 DIV.
(B-D) Graph shows the percentage of the PDGFαR-positive cells during the three analyzed time points in fetal (red line) and adult (blue line) cultures (B). The images show fetal (C) and adult (D) cultures at the end of the differentiation process (12 DIV).
(*E*-G) Graph shows the percentage of the NG2-positive cells during the three analyzed time points in fetal (red line) and adult (blue line) cultures (E). The images show the fetal (F) and adult (G) cultures at the end of the differentiation process (12 DIV).
(H-J) Graph shows the percentage of the CNPase-positive cells during the three analyzed time points in fetal (red line) and adult (blue line) cultures (H). The images show the fetal (I) and adult (J) cultures at the end of the differentiation process (12 DIV).
(K-M) Graph shows the percentage of the MBP-positive cells during the three analyzed time points in fetal (red line) and adult (blue line) cultures (K). The images show the fetal (N) and adult (M) cultures at the end of the differentiation process (12 DIV). Bar: 20 μm.
The bars represent the mean value ± SEM; n = three independent experiments. Statistical analysis: Two-way ANOVA followed by Tukey's post-hoc. The asterisks represent the differences in expression at the same time point between the fetal and adult cultures (* $P < 0.5$; ** $P < 0.1$; *** $P < 0.01$; **** $P < 0.001$).
Abbreviations: CNPase, 2′,3′-cyclic nucleotide 3′-phosphodiesterase; MBP, myelin basic protein; NG2, chondroitin sulphate proteoglycan, neural/glial antigen 2; PDGFαR, platelet derived growth factor alpha receptor. (For interpretation of the references to color in this figure legend, the reader is referred to the web version of this article.)

The reduced OL differentiation of OPCs derived from adult brain was not due to the altered cell fate of differentiating NSCs, since populations of NSC-derived astrocytes and neurons were not affected by age, as illustrated by a similar percentage of GFAP-positive cells (around 40%), and a small percentage of neurons (fetal, 5%; adult, 1%) in both cell cultures at the end of the differentiation phase (*data not shown)*. Moreover, no differences in total cell death or lineage-specific cell death, based on nuclear morphology, was detected between fetal and adult cultures (*data not shown*).

3.4. Fetal and adult NSCs-derived OPCs need RXRγ to differentiate in mature OLs

Considering the heavily compromised generation of mature OLs into adult vs fetal cultures, we investigated the process of maturation using APC alone and in combination with *Olig1* and *Olig2,* and re-evaluated the number of mature myelinating OLs in fetal and adult cultures using MBP. In addition, to study the role of RXRγ in this process, a NR significantly downregulated in adult precursors, we isolated NSCs from the fetal and adult brain of RXRγ+/+ and RXRγ−/− mice, using the same isolation and differentiation protocol as previously described (Fig. 5A).

The percentage of maturing and myelinating cells were strongly reduced in cultures isolated from RXRγ−/− animals irrespective of age (Fig. 5B. APC-positive cells; fetal, RXRγ−/− $p < 0.0083$; adult RXRγ−/− $p < 0.0001$), as can be seen in the images of the cultures (Fig. 5D, H and E, I). As a consequence, significantly fewer myelinating OLs were detected using MBP immunolabeling in both fetal and adult RXRγ−/− cultures (Fig. 5C; $p < 0.0001$ for fetal – Fig. 5F, J - and adult – Fig. 5G, K). Surprisingly, no significant differences in APC-positive cells appeared between fetal and adult RXRγ+/+ cultures (Fig. 5B). Considering that the number of mature myelinating OLs expressing MBP is lower in adult RXRγ+/+ cultures (Fig. 5C), this may suggest a delay in OL maturation in adult cultures.

Since generation of myelinated mature OLs from RXRγ−/− OPCs is compromised, we sought to determine the stage of OPC differentiation at which such impairment occurs. Furthermore, reduced expression of RXRγ in adult vs fetal precursors could also underlie deficient or delayed differentiation/maturation of adult OPCs. To investigate this hypothesis, we compared the progression of differentiation and maturation specific to adult and RXRγ−/− OPCs. To this end, we used the anti-APC antibody, in combination with the detection of *Olig1* and *Olig2*, which permitted us to discriminate between the differentiating OPCs and OLs at different stages of maturation. In the early phases, the OPCs are APC and *Olig1* negative, but positive for *Olig2*. APC-positive cells can be divided into Olig1-/Olig2+, Olig1+/Olig2+ and Olig1-/Olig2+ in an increasing level of maturation (Nakatani et al., 2013).

In contrast to a significant reduction in the number of APC-positive cells (OLs in maturation) in RXRγ−/− cultures, the percentage of APC- and Olig1-negative OPCs expressing Olig2+ was significantly increased in fetal, but not in adult RXRγ−/− cultures. In fact, the percentage of undifferentiated OPCs detected with this approach in fetal RXRγ−/− was not significantly different from the number of OPCs in adult wild type and RXRγ−/− cultures, whereas adult cultures displayed higher percentage of OPCs compared to fetal cultures (Fig. 5L, $p = 0.0062$), in agreement with the previous observation (Fig. 4B–G),.

Moreover, the analysis of the APC+ cells showed that, in agreement with the previous observation (see Fig. 5 C, F-K and 4H-M), adult RXRγ+/+ cultures displayed a lower percentage of mature OLs compared to fetal cultures, as identified by APC+/Olig1+/Olig2- ($p = 0.0095$). Furthermore, as expected, the first step of OL differentiation (APC+/Olig1-/Olig2+) was affected in adult cultures, which showed a higher percentage compared to fetal cultures ($p = 0.0004$). On the other hand, a very similar pattern was observed in RXRγ−/− cultures, although only fetal cultures showed an increase of APC+/Olig1-/Olig2+, corresponding to the early phases of maturation ($p = 0.0483$). Thus, although a lower number of RXRγ−/− OPCs differentiate, these cells show a similar maturation pattern, comparable to both fetal and adult RXRγ+/+ cultures.

Since progression in the differentiation progression cannot explain the deficits in generation of mature OLs in RXRγ−/− we addressed the possibility that RXRγ−/− OPCs do not enter the differentiation process.

3.5. RXRγ is involved in the T3-mediated cell cycle exit

To investigate the possible role of the RXRγ receptor in regulating the expression of key genes involved in OLs maturation and in the cell cycle exit, we isolated fetal cells from RXRγ−/− and RXRγ+/+ mice (Fig. 6A). Fetal cultures of NSC-derived OPCs were lysed before adding T3 (0 h), and 6 and 24 h after the T3-differentiation induction. Although no differences in expression levels were detected in TRα1, TRβ, Olig1, Olig2 or Klf9 expression (Supplemental Fig. 2S), enormous differences were detected in the expression of the p27, cMyc and PDGFαR genes (Fig. 6B). In particular, p27 is a gene directly regulated by T3, and is one of the main players in the T3-mediated cell cycle exit (Tokumoto et al., 2002). Expression of p27 increases after 24 h of T3 exposure in RXRγ+/+ cultures (RXRγ+/+ 0 vs. 24 h, $p = 0.0003$), while no changes were detected in RXRγ−/− cells (RXRγ+/+ vs RXRγ−/− at 24 h, $p = 0.0024$). cMyc is also known to be downregulated in oligodendrocytes by T3 action, leading to downstream activation of several genes related to the cell cycle exit (i.e. Cdc2 and H2afz; Magri et al., 2014). In fact, its expression decreased after 24 h of T3 exposure in RXRγ+/+ cultures (RXRγ+/+ 0 vs. 24 h, $p = 0.0396$), while no changes were detected in RXRγ−/− cells (RXRγ+/+ vs RXRγ−/− at 24 h, $p = 0.0472$). These gene expression analyses results suggest a block of RXRγ−/− OPCs in the precursor state, without any action of T3 in the cell cycle exit. This hypothesis is corroborated by

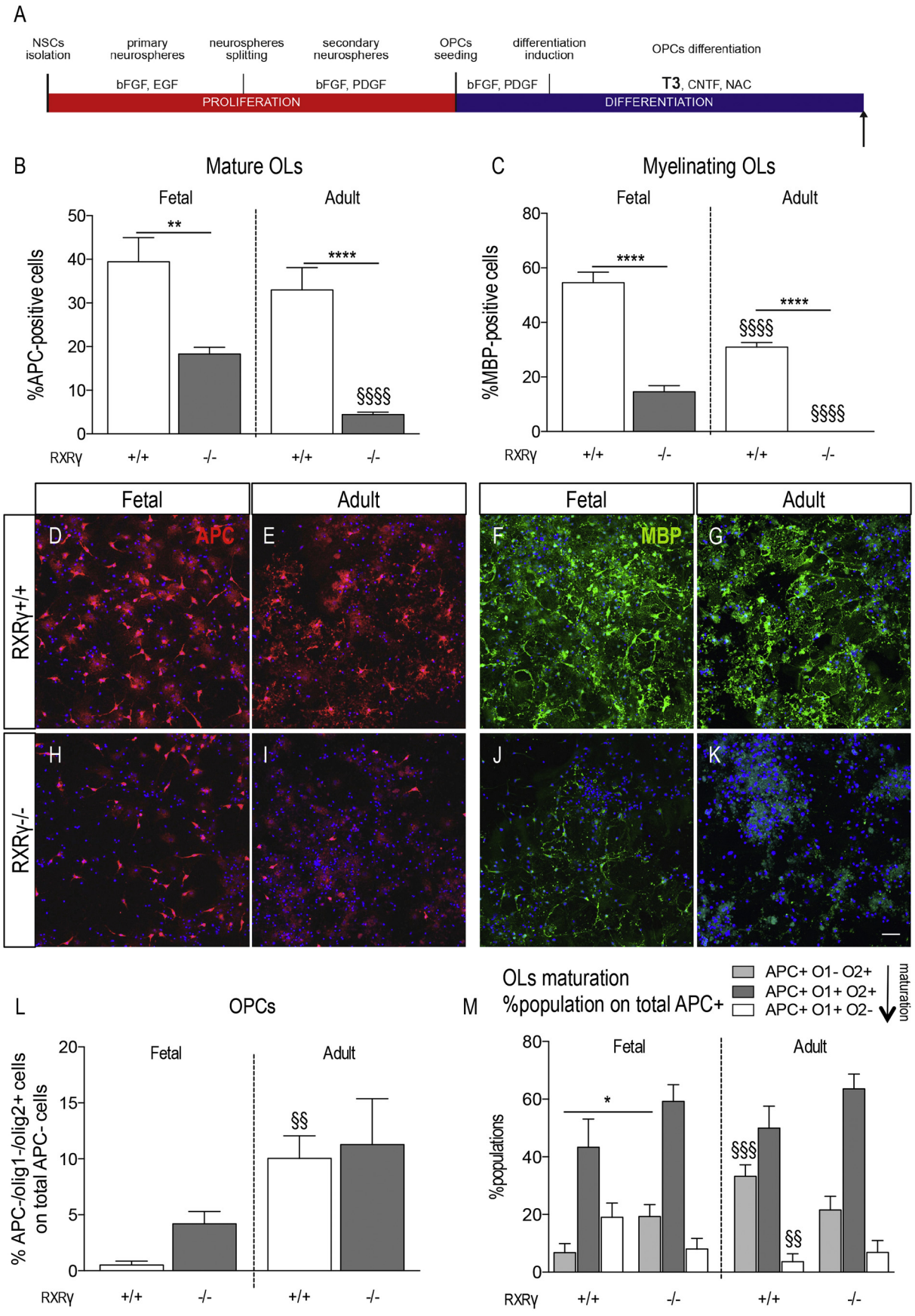

(caption on next page)

Fig. 5. Effect of RXRγ gene knock out in NSCs-derived OPCs differentiation.
(A) Experimental design: cell morphology and OL marker expression were analyzed in RXRγ+/+ and RXRγ−/− NSC-derived OPC cultures at the end of the differentiation process. The arrow shows the time point of the analysis: 12 DIV.
(B-C) The graphs show the percentage of APC-positive (B) and MBP-positive (C) cells in RXRγ+/+ (white column) and RXRγ−/− (grey column), fetal and adult cultures.
(D-K) The images show APC- (D, E, H, I) and MBP- (F, G, J, K) stained cells in RXRγ+/+ (D-G) and RXRγ −/− (H-K), in fetal (D, H, F, J) and adult (E, I, G, K) cultures. Bar: 50 μm.
(L) Graph shows the OPC population analysis, based on the APC/Olig1/Olig2 staining. Olig1-/Olig2+ cells are calculated from the total APC- cells, showing the percentage of immature OPCs.
(M) Graph shows the OLs maturation analysis, based on the APC/Olig1/Olig2 staining. The cells are divided in three different populations, with a growing degree of maturation: APC+/Olig1-/Olig2+; APC+/Olig1+/Olig2+ and APC+/Olig1+/Olig2-; measured from the total APC+ cells.
The bars represent the mean value ± SEM; n = three independent experiments. Statistical analysis: Student's *t*-test. The asterisks represent the differences between RXRγ−/− and RXRγ+/+ groups (* $p < 0.05$, *** $p < 0.001$, **** $p < 0.0001$); § represents the differences between the fetal and adult groups of the same genotype (§§ $p < 0.01$; §§§ $p < 0.001$; §§§§ $p < 0.0001$).
Abbreviations. APC, anti-adenomatous polyposis coli; MBP, Myelin basic protein; O1 (Olig1), Oligodendrocyte transcription factor 1; O2 (Olig2), Oligodendrocyte transcription factor 2; OLs, oligodendrocytes.

PDGFαR expression, related to the precursor state, which decreases in RXRγ+/+ OPCs at 6 and 24 h after T3 exposure (6 h, $p = 0.0005$; 24 h, $p = 0.0012$). In contrast, PDGFαR gene expression is not decreased by T3 exposure in RXRγ−/−, while it increases after 24 h (RXRγ−/− 0 vs. 24 h, $p < 0.0001$; RXRγ+/+ vs. RXRγ−/− at 24 h, $p < 0.0001$).

T3 is the best-known differentiating agent in OPCs, being the key regulator of the cell cycle from undifferentiated precursors (Billon et al., 2001). Thus, in order to analyze the effect of RXRγ gene ablation in cell cycle regulation, we measured the percentage of OPCs generated from cells isolated from the whole fetal forebrain of RXRγ−/− and RXRγ+/+ mice, following 24 h of T3-mediated differentiation, compared with cultures that were not treated with T3. However, RXRγ−/− cultures show a higher number of NG2-positive cells at the end of the differentiation phase, compared to RXRγ+/+ cultures ($p < 0.0001$; Fig. 6C–E), suggesting a possible dysregulation of the T3-induced cell cycle exit.

Cells were then stained for PDGFαR to identify OPCs, and for Ki67 to identify replicating cells. T3 induces a reduction in Ki67-positive OPCs, compared to RXRγ+/+ cultures treated with a vehicle ($p = 0.0486$). RXRγ−/− cultures show a higher percentage of replicating-OPCs compared to RXRγ+/+ ($p = 0.0315$). Moreover, the percentage of Ki67-positive OPCs is not affected by T3 treatment, and the level of OPCs remains higher, compared to the RXRγ+/+ cells treated with T3 ($p < 0.0001$; Fig. 6F–J).

4. Discussion

In spite of the fact that most of the OPCs populating the mature CNS are developmentally derived, the fetal and adult OPCs show substantial differences in molecular and biological properties.

In this study, we investigated the differentiation process of OPCs obtained from NSCs derived from fetal and adult brain, focusing on the role of NRs as key determinants of differentiation. This cell system was preferred to primary and purified OPCs to better mimic the developmental biology of OPCs, and in particular the lineage specification and subsequent proliferation/survival and maturation. In a previous study, we demonstrated that Poly (ADP-ribose) polymerase, an enzyme involved in cell viability and NRs expression, has a completely different role in fetal and adult OPCs (Baldassarro et al., 2017). Moreover, in vivo and in vitro studies indicate that OPCs exhibit different properties according to their chronological age (Cui et al., 2012), and that adult OPCs have a longer cell cycle than perinatal OPCs (Tang et al., 2000), corroborating the hypothesis that the two OPCs have different characteristics and maturation potential.

We showed that (i) the mRNA expression level of several NRs and co-regulators is different in fetal and adult NSCs and OPCs at comparable differentiation stages; (ii) adult NSCs-derived OPCs have a different yield of maturation compared to fetal-derived OPCs; (iii) lower expression of *RXR*γ in adult NSCs underlies fetal/adult differences in differentiation potential, and iv) this effect is probably related to cell cycle exit.

4.1. NR signaling in fetal vs adult OPC

NRs play key roles in all the differentiation stages of OLs, from NSC self-renewal and lineage specification, to OPC cell cycle exit and OL maturation (Mendoza and Hollenberg, 2017).

Here we showed that NSCs derived from the SVZ of the adult brain display a much higher *TRβ* and a lower *RXR*γ mRNA expression level than NSCs derived from fetal brain. These differences correlate with a higher expression level of *Olig1*, *Olig2* and *Klf9* mRNAs in adult derived OPCs at early stages of the differentiation process. Olig1 and Olig2 are closely related transcription factors which play critical roles in OL specification and differentiation. The expression of the two *Oligs* is temporally regulated, with a later expression of *Olig1*, inducing the expression of mature OLs genes (MBP and PLP1; Maijer et al., 2012), while *Klf9* is a T3-target gene, which is critically involved in OPC maturation and directly induced by T3 (Dugas et al., 2012). The higher expression of these genes reflects a more mature phenotype in adult-derived OPCs at early stages, and may result in a lower response to the T3-mediated differentiation stimulus.

This different expression profile might indicate a reduced capacity to differentiate in adult-derived NSCs. In fact, it has already been described that TRβ has specific roles in fetal and adult NSCs (Gkikas et al., 2017), while no data is available for the role of RXRγ in adult-derived NSCs (Takouda et al., 2017). Moreover, RXRγ expression also remains lower in adult mature/myelinating OLs compared to fetal.

On the other hand, the role of T3 in mediating the differentiation process in OPCs is well-established, acting as ligand for α and β TR isotypes to control transcription target genes (Billon et al., 2002). We showed that both adult and fetal cell systems need T3 to differentiate, but that fetal cells are more responsive to T3-induced differentiation, as indicated by a higher level of differentiation markers (*Olig1*, *Olig2*, *Klf9*), and by the higher number of MBP-positive OLs. Moreover, the morphological phenotype of CNPase and MBP-positive cells is more mature in fetal OPCs, suggesting a possible delay in the differentiation of the adult-derived cells. These differences support the view that T3 action on the differentiation process of OPCs depends on the age of the animal, and supports previous observations that T3-dependent gene expression regulation is spatially and temporally regulated (Astapova, 2016).

4.2. RXRγ involvement in T3-mediated OPC cell cycle exit

Overexpression of *TRβ* and reduced expression of *RXR*γ in adult NSCs may reflect the reduced differentiation/maturation potential of adult cells. In fact, according to the classical experiments by Raff and collaborators (Billon et al., 2001), T3 drives the OPC out from the cell

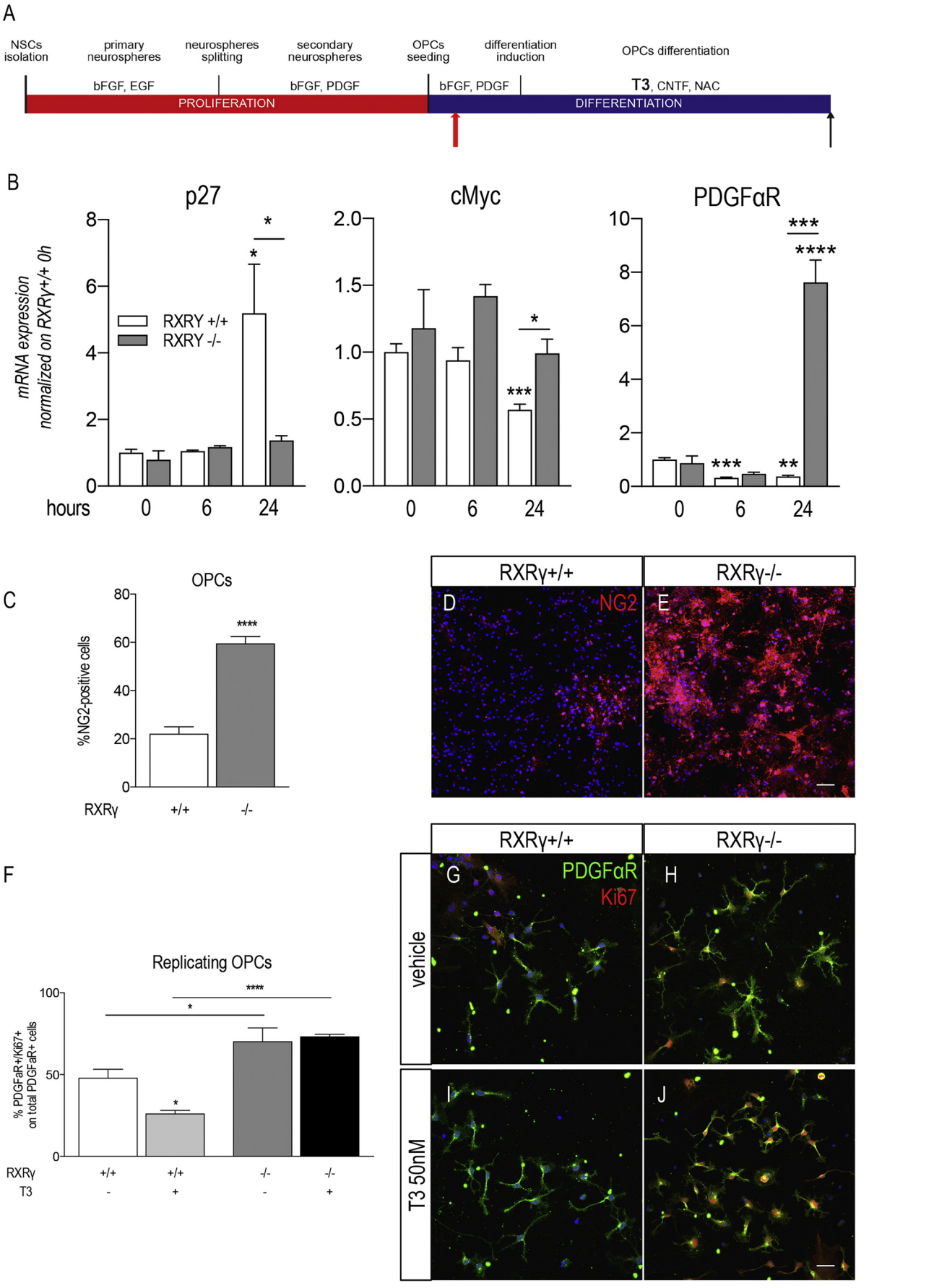

(caption on next page)

Fig. 6. RXRγ role in differentiation and cell cycle.
(A) Experimental design. Fetal RXRγ+/+ and RXRγ−/− culture gene expression was analyzed 0, 6 and 24 (red arrow) hours after T3-induced differentiation. At the last time point (red arrow), cells were also fixed and stained for PDGFαR and Ki67 in order to analyze the percentage of replicating OPCs. At the end of the differentiation process, the cells were fixed and analyzed for the percentage of NG2-positive cells in the culture (black arrow).
(B) Gene expression analysis of three key genes involved in OPCs cell cycle exit: p27, cMyc and PDGFαR.
(C-E) Graph shows the percentage of NG2-positive cells at the end of the differentiation process (12 DIV) in fetal RXRγ+/+ and RXRγ−/− cultures (C). The images show RXRγ+/+ (D) and RXRγ−/− (E) NG2-stained cultures. Bar: 50 μm.
(F-J) Graph shows the percentage of double positive PDGFαR/Ki67 cells of the total number of PDGFαR-positive cells, in vehicle- and T3-treated, RXRγ+/+ and RXRγ−/− cultures (F). The images show vehicle- (G, H) and T3- (I, J) treated, RXRγ+/+ (G, I) and RXRγ−/− (H, J) cultures. Bar: 20 μm.
The bars represent the mean value ± SEM; n = three independent experiments. Statistical analysis: Two-way ANOVA followed by Tukey's post-hoc (B), Student's t-test (C), One-way ANOVA followed by Tukey's post-hoc (F). The asterisks represent the differences between RXRγ−/− and RXRγ+/+ groups (* $P < 0.05$, **** $P < 0.0001$). In graph B, where not indicated by the horizontal line, the asterisks represent the differences between 0 h and other time points in the same genotype. In graph F, where not indicated by the horizontal line, the asterisks represent the differences in the same genotype.
Abbreviations: cMyc, bHLH transcription factor; *NG2, chondroitin sulphate proteoglycan, neural/glial antigen 2; Olig1, Oligodendrocyte transcription factor 1; Olig2, Oligodendrocyte transcription factor 2; p27, Cyclin-dependent kinase inhibitor 1B; PDGFαR, platelet derived growth factor alpha receptor; TRα1, Thyroid hormone receptor alpha 1; TRβ, thyroid hormone receptor beta.* (For interpretation of the references to color in this figure legend, the reader is referred to the web version of this article.)

cycle after a defined number of cell replications (Perez-Juste and Aranda, 1999), and is also needed to start differentiation (Tokumoto et al., 2002), directly regulating different proteins involved in cell cycle control (Puzianowska-Kuznicka et al., 2006). Thus, enhanced *TRβ* expression may instead increase the differentiation potential of NSCs and reduce the number of progenitor divisions prior to terminal differentiation in adult-derived NSCs. Alternatively, a limited amount of RXRγ could be the limiting factor for TRβ activity and thus reduce responsiveness to T3, even in the presence of higher levels of TRβ expression. Indeed, in addition to TRs, the activation of RXRs by pharmacological and genetic manipulation stimulates OL differentiation by enhancing remyelination (Huang et al., 2011; de la Fuente et al., 2015), and the TR/RXR heterodimer is proposed as being the primary mediator of the target gene regulation by T3 (Lee and Privalsky, 2005). Moreover, an up-regulation of the RXRγ mRNA expression level has been described during remyelination (Huang et al., 2011), being expressed in OLs in remyelinating lesions in mouse CNS, and in tissue from individuals with multiple sclerosis (MS), a disease characterized by extensive demyelination and remyelination phases.

To address the functional relevance of reduced RXRγ in early precursors derived from adult brain in terms of their differentiation and maturation capacity, we investigated the T3-induced OL differentiation of NSCs derived from fetal and adult RXRγ null mutant mice as a model of compromised RXRγ signaling, and found that the lack of RXRγ severely impairs the overall number of mature, myelinating RXRγ−/− OLs. Such a deficit may, to some extent, result from delayed maturation, since the percentage of OLs at an early phase of maturation (APC+, Olig1-, Olig2+) showed an increase in RXRγ−/− in fetal cultures. Importantly, a similar increase in APC+, Olig1-, Olig2+, and OLs was also observed in adult- compared to fetal-derived cells, suggesting a delay in OL maturation in adult cultures. Another check-point controlled by RXRγ and affected in adult OPC differentiation is cell cycle exit. Several lines of evidence support the possibility that cell cycle exit is compromised in RXRγ−/− OPCs: (i) an overall reduction of APC-positive OLs undergoing maturation, (ii) a concomitant higher number of NG2-positive OPCs in RXRγ−/− fetal cultures, (iii) and an increased number of PDGFαR/Ki67 double-positive cells corresponding to replicating OPCs in RXRγ−/− cultures 24 h after the T3- differentiation induction.

Importantly, a similar reduced capacity to exit cell cycle was also displayed by adult-derived OPCs, as indicated by an increased number of NG2- or PDGFαR- positive OPCs at the end of the differentiation process, and a concomitant decrease in MBP-positive myelinating OLs.

Moreover, despite the fact that certain genes involved in OPC maturation do not show differential expression in RXRγ−/− cells (Olig1, Olig2, TRα1, TRβ and Klf9), key genes involved in the cell cycle exit are dysregulated in the absence of RXRγ. In particular, p27 and cMyc, whose expressions need to be increased and decreased respectively due to T3-mediated maturation induction (Tokumoto et al., 2002; Magri et al., 2014), remain stable in RXRγ−/− cells, proving the role of this receptor in mediating T3 action on cell cycle exit. In fact, together with the higher percentage of NG2-positive cells at the end of the differentiation phase in RXRγ−/− cells, these cells do not show a decrease in PDGFαR expression following 6 and 24 h of T3 exposure as RXRγ+/+ cells do, instead increasing in expression after 24 h.

5. Conclusions

In conclusion, we showed that adult NSCs show a higher expression of *TRβ* and lower expression of *RXRγ* compared to fetal cells, and that such differences correlate with a reduced capacity to generate mature, myelinating OLs from adult NSCs-derived OPCs in the T3-mediated differentiation process. We also show that the lower potential of adult NSCs for oligodendrogenesis may reflect a mostly delayed maturation process, but also a reduced capacity to exit the cell cycle. Through studies of RXRγ−/− mice, we provide evidence that the decreased expression of RXRγ is an important determinant of these differences, as indicated by the heavily compromised differentiation of fetal RXRγ−/− NSCs, and the complete absence of mature myelinating OLs in cultures from adult RXRγ−/− NSCs. Mechanisms of such deficits primarily reflect the role of RXRγ in controlling cell cycle exit during OPC differentiation in response to T3 stimulation, and delayed maturation.

Acknowledgements

This work was funded by the ARSEP Foundation as part of the project “Role of RXRγ in T3-mediated oligodendrocytes differentiation and remyelination”.

This work was partially funded by the IRET Foundation, Ozzano Emilia, Italy (no-profit organization), as part of the “Step-by-Step” POR-FESR 2016-2020 Emilia Romagna Region project.

LabEx ANR-10-LABX-0030-INRT, a French State fund managed by the Agence Nationale de la Recherche as part of the program Investissements d'Avenir ANR-10-IDEX-0002-02 also contributed to funding.

All authors declare that they have no conflict of interest.

Declarations of interest

None.

Authors contribution

VAB: performed the experiments, contributed to study design and wrote the manuscript.

WK: contributed to the study design and wrote the manuscript.

MF: performed qPCR analysis.

BS: management and genotyping of RXRγ-/- mice.

LG: ideated and designed the study.
LC: ideated and designed the study and wrote the manuscript.

Appendix A. Supplementary data

Supplementary data to this article can be found online at https://doi.org/10.1016/j.scr.2019.101443.

References

Alhenius, H., Kokaia, Z., 2010. Isolation and generation of neurosphere cultures from embryonic and adult mouse brain. Methods Mol. Biol. 633, 241–252.

Astapova, I., 2016. Role of co-regulators in metabolic and transcriptional actions of thyroid hormone. J. Mol. Endocrinol. 56, 73–97.

Baldassarro, V.A., Marchesini, A., Giardino, L., Calzà, L., 2017. PARP activity and inhibition in fetal and adult oligodendrocyte precursor cells: effect on cell survival and differentiation. Stem Cell Res. 22, 54–60.

Baxi, E.G., Schott, J.T., Fairchild, A.N., Kirby, L.A., Karani, R., Uapinyoying, P., Pardo-Villamizar, C., Rothstein, J.R., Bergles, D.E., Calabresi, P.A., 2014. A selective thyroid hormone β receptor agonist enhances human and rodent oligodendrocyte differentiation. Glia 62, 1513–1529.

Bengtsson, S.L., Nagy, Z., Skare, S., Forsman, L., Forssberg, H., Ullen, F., 2005. Extensive piano practicing has regionally specific effects on white matter development. Nat. Neurosci. 8, 1148–1150.

Bercury, K.K., Macklin, W.B., 2015. Dynamics and mechanisms of CNS myelination. Dev. Cell 32, 447–458.

Billon, N., Tokumoto, Y., Forrest, D., Raff, M., 2001. Role of thyroid hormone receptors in timing oligodendrocyte differentiation. Dev. Biol. 235, 110–120.

Billon, N., Jolicoeur, C., Tokumoto, Y., Vennstrom, B., Raff, M., 2002. Normal timing of oligodendrocyte development depends on thyroid hormone receptor alpha 1 (TRalpha1). EMBO J. 21, 6452–6460.

Billon, N., Terrinoni, A., Jolicoeur, C., McCarthy, A., Richardson, W.D., Melino, G., Raff, M., 2004. Roles for p53 and p73 during oligodendrocyte development. Development 131, 1211–1220.

Bradl, M., Lassmann, H., 2010. Oligodendrocytes: biology and pathology. Acta Neuropathol. 119, 37–53.

Calzà, L., Baldassarro, V.A., Fernandez, M., Giuliani, A., Lorenzini, L., Giardino, L., 2017. Thyroid hormone and the white matter of the central nervous system: from development to repair. Vitam. Horm. 106, 253–280.

Casaccia-Bonnefil, P., Liu, A., 2003. Relationship between cell cycle molecules and onset of oligodendrocyte differentiation. J. Neurosci. Res. 72, 1–11.

Chen, Y., Balasubramaniyan, V., Peng, J., Hurlock, E.C., Tallquist, M., Li, J., Lu, Q.R., 2007. Isolation and culture of rat and mouse oligodendrocyte precursor cells. Nat. Proc. 2, 1044–1051.

Crawford, A.H., Chambers, C., Franklin, R.J., 2013. Remyelination: the true regeneration of the central nervous system. J. Comp. Pathol. 149, 242–254.

Cui, Q.L., D'Abate, L., Fang, J., Leong, S.Y., Ludwin, S., Kennedy, T.E., Antel, J., Almazan, G., 2012. Human fetal oligodendrocyte progenitor cells from different gestational stages exhibit substantially different potential to myelinate. Stem Cells Dev. 21, 1831–1837.

de la Fuente, A.G., Errea, O., van Wijngaarden, P., Gonzales, G.A., Kerninon, C., Jarjour, A.A., Lewis, H.J., Jones, C.A., Nait-Oumesmar, B., Zhao, C., Huang, J.K., fFrench-Constant, C., Franklin, R.J., 2015. Vitamin D receptor-retinoid X receptor heterodimer signaling regulates oligodendrocyte progenitor cell differentiation. J. Cell Biol. 211, 975–985.

Dietz, K.C., Polanco, J.J., Pool, S.U., Sim, F.J., 2016. Targeting human oligodendrocyte progenitors for myelin repair. Exp. Neurol. 283, 489–500.

Dugas, J.C., Ibrahim, A., Barres, B.A., 2012. The T3-induced gene KLF9 regulates oligodendrocytes differentiation and myelin regeneration. Mol. Cell. Neurosci. 50, 45–57.

Durand, B., Raff, M., 2000. A cell-intrinsic timer that operates during oligodendrocyte development. Bioessays. 22, 64–71.

Franklin, R.J.M., Hinks, G.L., 1999. Understanding CNS remyelination: clues from developmental and regeneration biology. J. Neurosci. Res. 58, 207–213.

Fukushima, S., Nishikawa, K., Furube, E., Muneoka, S., Ono, K., Takebayashi, H., Miyata, S., 2015. Oligodendrogenesis in the fornix of adult mouse brain; the effect of LPS-induced inflammatory stimulation. Brain Res. 1627, 52–69.

Gkikas, D., Tsampoula, M., Politis, P.K., 2017. Nuclear receptors in neural stem/progenitor cell homeostasis. Cell. Mol. Life Sci. 74, 4097–4120.

Goldman, S.A., Kuypers, N.J., 2015. How to make an oligodendrocyte. Development 142, 3983–3995.

Hill, R.A., Li, A.M., Grutzendler, J., 2018. Lifelong cortical myelin plasticity and age-related degeneration in the live mammalian brain. Nat. Neurosci. 21, 683–695.

Huang, J.K., Jarjour, A.A., Nait Oumesmar, B., Kernion, C., Williams, A., Krezel, W., Kagechika, H., Bauer, J., Zhao, C., Baron-Van Evercooren, A., Chambon, P., Ffrench-Constant, C., Franklin, R.J.M., 2011. Retinoid X receptor gamma signaling accelerates CNS remyelination. Nat. Neurosci. 14, 45–53.

Hughes, E.G., Kang, S.H., Fukaya, M., Bergles, D.E., 2013. Oligodendrocyte progenitors balance growth with self-repulsion to achieve homeostasis in the adult brain. Nat. Neurosci. 16, 668–676.

Kessaris, N., Fogarty, M., Iannarelli, P., Grist, M., Wegner, M., Richardson, W.D., 2006. Competing waves of oligodendrocytes in the forebrain and postnatal elimination of an embryonic lineage. Nat. Neurosci. 9, 173–179.

Krezel, W., Dupé, V., Mark, M., Dierich, A., Kastner, P., Chambon, P., 1996. RXR gamma null mice are apparently normal and compound RXR alpha +/−/RXR beta −/−/RXR gamma −/− mutant mice are viable. Proc. Natl. Acad. Sci. U. S. A. 93, 9010–9014.

Lee, J.Y., Petratos, S., 2016. Thyroid hormone signaling in oligodendrocytes: from extracellular transport to intracellular signal. Mol. Neurobiol. 53, 6568–6583.

Lee, S., Privalsky, M.L., 2005. Heterodimers of retinoic acid receptors and thyroid hormone receptors display unique combinatorial regulatory properties. Mol. Endocrinol. 19, 863–878.

Magri, L., Gracias, M., Wu, M., Swiss, V.A., Janssen, W.G., Casaccia, P., 2014. C-Myc-dependent transcriptional regulation of cell cycle and nucleosomal histones during oligodendrocyte differentiation. Neurosci. 12, 72–86.

Maijer, D.M., Kane, M.F., Mehta, S., Liu, H., Harrington, E., Taylor, C.M., Stiles, C.D., Rowitch, D.H., 2012. Separated at birth? The functional and molecular divergence of OLIG1 and OLIG2. Nat. Rev. Neurosci. 13, 819–831.

Marin, M.A., Carmichael, S.T., 2018. Mechanisms of demyelination and remyelination in the young and aged brain following white matter stroke. Neurobiol. Dis. https://doi.org/10.1016/j.nbd.2018.07.023.

Mendoza, A., Hollenberg, A.N., 2017. New insights into thyroid hormone action. Pharmacol. Ther. 173, 135–145.

Michalski, J.P., Kothary, R., 2015. Oligodendrocytes in a nutshell. Front. Cell. Neurosci. 9, 1–11.

Nakatani, H., Martin, E., Hassani, H., Clavairoly, A., Maire, C.L., Viadieu, A., Kerninon, C., Delmasure, A., Frah, M., Weber, M., Nakafuku, M., Zalc, B., Thomas, J.L., Guillemot, F., Nait-Oumesmar, B., Parras, C., 2013. Ascl1/Mash1 promotes brain oligodendrogenesis during myelination and remyelination. J. Neurosci. 33, 9752–9768.

Perez-Juste, G., Aranda, A., 1999. The cyclin-dependent kinase inhibitor p27(Kip1) is involved in thyroid hormone-mediated neuronal differentiation. J. Biol. Chem. 274, 5026–5031.

Puzianowska-Kuznicka, M., Pietrzak, M., Turowska, O., Nauman, A., 2006. Thyroid hormones and their receptors in the regulation of cell proliferation. Acta Biochim. Pol. 53, 641–650.

Schlegel, A.A., Rudelson, J.J., Tse, P.U., 2012. White matter structure changes as adults learn a second language. J. Cogn. Neurosci. 24, 1664–1670.

Takouda, J., Katada, S., Nakashima, K., 2017. Emerging mechanisms underlying astrogenesis in the developing mammalian brain. Proc. Jpn. Acad Ser. B. Phys. Biol. Sci. 93, 386–398.

Tang, D.G., Tokumoto, Y.M., Raff, M.C., 2000. Long-term culture of purified postnatal oligodendrocyte precursor cells. Evidence for an intrinsic maturation program that plays out over months. J. Cell Biol. 148, 971–984.

Tokumoto, Y.M., Apperly, J.A., Gao, F.B., Raff, M.C., 2002. Posttranscriptional regulation of p18 and p27 Cdk inhibitor proteins and the timing of oligodendrocyte differentiation. Dev. Biol. 245, 224–234.

Urbán, N., Guillemot, F., 2014. Neurogenesis in the embryonic and adult brain: same regulators, different roles. Front. Cell. Neurosci. 8, 396.

Viganò, F., Dimou, L., 2016. The heterogeneous nature of NG2-glia. Brain Res. 1638, 129–137.

Yeung, M.S., Zdunek, S., Bergmann, O., Bernard, S., Salehpour, M., Alkass, K., Perl, S., Tisdale, J., Possnert, G., Brundin, L., Druid, H., Frisén, J., 2014. Dynamics of oligodendrocyte generation and myelination in the human brain. Cell 159, 766–774.